Wind Energy

WIND ENERGY
Wind Energ. (2017)
Published online in Wiley Online Library (wileyonlinelibrary.com). DOI: 10.1002/we.2078

RESEARCH ARTICLE

Low wind speed events: persistence and frequency

Platon Patlakas[1], George Galanis[1,2], Dimitris Diamantis[1] and George Kallos[1]

[1] Department of Physics, Atmospheric Modeling and Weather Forecasting Group, University of Athens, University Campus, Bldg. PHYS-V, Athens 15784, Greece
[2] Section of Mathematics, Hellenic Naval Academy, Hatzikiriakion, Piraeus 18539, Greece

ABSTRACT

Over the last decades, wind energy industry has been growing with an increasing rate. This is highly relevant to the need of new wind farm site selection with certain standards such as high wind potential and accessibility. Even in windy areas, low wind speed persistence can be characterized as an extreme (non-frequent) atmospheric condition for the electricity network as it can lead to low or no energy production. The current work is focused on the estimation of the duration and the frequency of occurrence of low wind speed events using the principles of extreme value theory. The two methods used are the 'intensity given duration' and the 'duration given intensity' that lead to the same point from different perspectives. The data used is derived from a 10 year, hindcast, high-resolution database developed by the Atmospheric Modeling and Weather Forecasting Group of the University of Athens. The great potential and multinational interest concerning energy applications in the North Sea has led to its selection as a study area. The outcome of the study includes the development of intensity–duration–frequency curves as well as a comparison between the two methodologies adopted. Based on these, the largest period of no energy production for a preselected probability of occurrence is estimated for the area of interest. The results of this work could be potentially supportive for studying the regional climatology. Such information can be included in risk assessment techniques and can be applied among others for energy activities. Copyright © 2017 John Wiley & Sons, Ltd.

KEYWORDS

energy; extremes; intensity–duration–frequency curves; low wind speed; regional climatology; site assessment; wind energy

Correspondence

George Kallos, Department of Physics, Atmospheric Modeling and Weather Forecasting Group, University of Athens, University Campus, Bldg. PHYS-V, Athens 15784, Greece.
E-mail: kallos@mg.uoa.gr

Received 8 March 2016; Revised 21 November 2016; Accepted 30 November 2016

1. INTRODUCTION

Wind farm siting is approached today by generally accepted standards.[1] High wind potential and site accessibility are among the most important requirements. However, these cannot always be compatible, and this is the reason why risk assessment techniques are needed. These techniques usually take into consideration various parameters including the impact of wind speed in a wind power project. The study of the wind speed probability distribution main body and upper tail is used for the estimation of the energy potential and the extreme wind events that characterize the area under consideration.

A better understanding of the environmental resources behavior requires additional information that can be used towards a more integrated research in the field of wind farm siting. For this reason, apart from the mainstream approaches described shortly before, the concept of low wind speed event is introduced. The existence and the frequency of such events are positively correlated with the existence of high pressure systems. These systems are characterized by light winds at the surface, cover large areas and can last up to several days depending on the regional climate. This form of extreme conditions can cause several problems in electricity networks because several turbines are affected simultaneously.

There are more than one definitions of calm conditions related to light winds. It should be noted that different authors use various ways to define it and refer to a range of conditions. A characteristic example is the definition implied

by Smith.[2] According to this, calm conditions are specified when the mean wind speed is comparable with or less than the root-mean-square turbulent horizontal velocity. The present work is wind energy oriented. The cut in speed of a wind turbine has values normally around 3 m s^{-1}, depending on its type. For this reason, the threshold of 3 m s^{-1} is used here for the low wind speeds definition. However, the methodologies discussed in the following sections can be applied for different values.

Towards this direction, this study is focused on the duration and frequency of low wind speed events based on modeled wind speed time series. The main objective is to define the probability of occurrence of such events in terms of return periods and quantify the associated uncertainties. This estimation can be approached by using the principles of extreme value theory. For this purpose, two methods that lead to the same point by different perspectives are used, namely, 'intensity given duration' (IGD) and 'duration given intensity' (DGI). Different tools and probability distributions are tested in order to quantify the uncertainties employed from the use of these methodologies. The convergence of the final results is discussed, and the application in a wider area is tested.

Intensity given duration provides more information simultaneously if compared with DGI, as the results are expressed through intensity–duration–frequency (IDF) curves.[3] These are widely used in hydrology for the study of extreme precipitation events[4] or the frequency and the duration of droughts.[5] IDF curves can be used also in wave climate characterization describing the relationship between sea state intensity, sea state duration and frequency.[6] Considering wind, there is a variety of studies describing the upper tails of wind speed distribution in terms of return periods.[7–9] Studies about low wind speed events are quite few. Deaves and Lines[10] studied the frequency of low wind speed conditions oriented for risk assessments for hazardous installations. More specifically, they studied the effect of low winds on the dispersion of toxic or flammable gases. Continuing this work, Lines defined guidelines for the inclusion of low wind speed conditions into risk assessment techniques.[11] Gadian focuses on the directional persistence of low wind speed that can affect the dispersion of pollutants.[12] Another approach, introduced by Leahy and McKeogh,[13] is focused on the implications of low wind speed persistence in wind power and contains the concept of both IGD and DGI methodologies.

In the present study, for the application of DGI and IGD, annual maxima/minima (AM) method[14] was used for the extrapolation in time. The area under consideration is a part of the North Sea with rather high wind energy potential. This characteristic led the surrounding countries to take advantage of it and use it in energy applications.

The data employed in this work consists mainly of modeled time series, extracted from a database created by the Atmospheric Modeling and Weather Forecasting Group (AM&WFG—University of Athens) under the framework of Marina Renewable Integrated Application Platform (MARINA—Platform, http://forecast.uoa.gr/proj_marina.php,[15]). The use of the database has the advantage that wind speed values are available at different model levels/heights (here 80 m) and cover a large area without missing values. At the same time, the spatial coverage allows neighboring points on the spatial grid to be used to test elements of the methodology. More information about this database is provided in a following section (data used).

The provided output forms alternative information concerning the climatology of the study area that is not widely used. Such information can be included in risk assessment techniques and can be applied among others for energy activities.

2. METHODOLOGY APPLIED

The study of the existence and frequency of low wind speed events is based on two approaches, 'intensity given duration' and 'duration given intensity' method. In the following subsections, the basic facts and tools are discussed.

2.1. Intensity given duration

The application of this methodology requires the selection of a range of different durations/windows from 2 to 480 h (20 days, as a safe limit ensuring a big range of durations[13]). More specifically, maximum values mv_d of wind speed v_t are estimated over moving windows for each year:

$$\max\{v_t \ldots v_{t+d}\} = mv_d \text{ , where } t = \{1 \ldots \textit{total annual hours} - d\}; d = 2, \ldots, 480 \quad (1)$$

As a result, a new array (mv_d) with $n - d + 1$ components per year is obtained with cumulative distribution function (CDF) $F_u(u|d)$ and probability density function (PDF) $f_u(u|d)$, where u is the variable under study (here wind speed), n equals the total hours (of each year) and d represents the window length (in hours).

The next step is the adoption of a representative distribution for the extrapolation in time. The PDF and the CDF of the data will be denoted as $F_u(u|d;a,b,c,\ldots)$ and $f_u(u|d;a,b,c,\ldots)$, respectively. The parameters *a, b, c, ...* are highly dependent

DOI: 10.1002/we

on the given duration, the characteristics of the selected distribution and the method used for the distribution fit. The relation between the intensity, the duration and the frequency (return period- T_u) of the event is the following:

$$1 - \frac{\Delta t}{T_u} = F_u(u|d; a, b, c, \ldots) \tag{2}$$

where Δt is the time interval of the data to be fitted.

In the present study, the extrapolation will be based on the principles of extreme value theory and the use of annual maxima method as it is considered straight forward, and no decisions have to be made for its application.[7] The fitting distribution selected is Gumbel (minimum) as the desired outcome is the lowest value for a defined return period.[13] For this reason, there is the need for a new dataset, created by selecting the lowest value of the vector mv_d for each particular year. Because the database is 10 year long, the dataset will be constituted of 10 values in total. The new PDF and CDF are set as $F_u'(u|d;\alpha,\beta)$ and $f_u'(u|d;\alpha,\beta)$ respectively where α is the scale and β is the location parameter. At the same time, Δt in Equation (2) is equal to one as the values are annual. The given equation is transformed into the following:

$$1 - \frac{1}{T_u} = F_u'(u|d; \alpha, \beta) \tag{3}$$

The application of this method can be carried out by using different tools for the parameters estimation such as method of moments (MoM)[16,17] and maximum likelihood (ML) method.[16,18] Using these as well as the CDF of Gumbel (minimum) and Equation (3), the maximum value of a low wind speed event (U) of a given duration (D) can be extracted from:

$$U_D(T_u) = \alpha^* \left(\ln\left(-\ln\left(1 - \frac{1}{T_u} \right) \right) \right) + \beta \tag{4}$$

(Variable U corresponds to the wind speed threshold as defined in the following lines in DGI methodology.)

Applying different time windows will result to a matrix of the wind speed (U), the total duration (d) and the return period of the event (T_u) (all combined). The graphical representation of this matrix is made through the use of IDF curves.

The wind speed maximum intensity for a given return period can be related to the duration of the event by fitting a curve to the results. This curve is a function of the duration, which is found to be well represented by a second degree polynomial (5.1) or a logarithm function[13] (5.2):

$$U(D) = b\,D^2 + c\,D + d \tag{5.1}$$

$$U(D) = d + c\ \ ln(D) \tag{5.2}$$

In both cases, the parameters (b, c and/or d) are estimated using least squares method. In this study and for the selected area, polynomials were found to be more representative concerning lower speeds, which is the target.

2.2. Duration given intensity

This approach is based on the definition of a threshold. This threshold is set at 3 m s^{-1} in the present study, based on the cut-in wind speed for energy generators. The time windows that wind speed is constantly below the selected threshold are characterized as low wind (no production) periods. These cases can be identified by taking into consideration the threshold crossovers. The application of this methodology required the largest period of each year to be selected (annual maximum) for the creation of the dataset needed to apply annual maxima method. The distributions used for the dataset fit vary, while the parameter estimation method tested is ML. For the estimation of low wind speed periods with return period T_d years, the following relationship was used:

$$1 - \frac{1}{T_d} = F_d(d|u; \alpha, \beta, \gamma) \tag{6}$$

where α is the scale parameter, β is the location parameter and γ is the shape parameter.

Equation (6), combined with the CDF of the distributions under study, leads to the relationships for the estimation of the T-year duration of a low wind speed event.

The selected distributions belong to the generalized extreme distribution family. The use of them is common for the estimation of return periods, but it depends on the dataset characteristics (e.g., skewness) and the desired degrees of freedom (parameters of the distribution). The distributions used alongside with the equations for the estimation of the durations are as follows:

Gumbel (maximum) distribution:

$$D_u(T_d) = \beta - \alpha ln\left[-\ln\left(1-\frac{1}{T_d}\right)\right] \tag{7}$$

Generalized extreme value (GEV) distribution:

$$D_u(T_d) = \beta + \frac{a}{\gamma}\left\{1-\left[-\ln\left(1-\frac{1}{T_d}\right)\right]^{\gamma}\right\} \tag{8}$$

Weibull distribution:

$$D_u(T_d) = \alpha \ln(T_d)^{1/\gamma} \tag{9}$$

Rayleigh distribution:

$$D_u(T_d) = \sqrt{2\alpha^2 \ln(T_d)} \tag{10}$$

3. DATA USED

The area of interest is a part of the North Sea (51°-60°N, 5°W-15°E) that is illustrated in Figure 1 (marked by a red box). The choice of this location was made for its wind climate characteristics that favor the operation of offshore wind energy platforms.[19] The wind energy potential is rather high, and the surrounding countries are investing in it by installing wind generators. Wind climate over the North Sea is influenced by the 'Westerlies' that is a wind pattern between 30° and 60° latitude. Generally, the weather is characterized by relatively high winds as illustrated in Figure 2. The prevailing weather systems are associated with the lows generated in the North Atlantic region and move eastward. Less frequent synoptic systems are the so-called polar lows that are connected with strong wind conditions.

The source of data used for the study is derived from the MARINA database.[15] Wind speed of the third vertical level (80 m) of the atmospheric model used for the hindcast analysis is the quantity under consideration. The choice of this level is based on the fact that this is a direct output of the model (no interpolation needed) and corresponds to the height used in most of offshore wind generators. Concerning the mentioned database, one of the most important effects accounted for, was the coupling between wind and wave-induced processes using state-of-the-art modeling systems. More specifically, the regional atmospheric model SKIRON[20–22] is used for wind; the third-generation ocean wave model WAM[23,24] is used for wave and HYCOM[25] for currents. The coupled system, used for the present study, is a well-established model and successfully evaluated in various research works.[26–32] For the MARINA platform project, the models have been run at a relatively high spatial resolution of 0.05° × 0.05° latitude/longitude covering a large part of Europe, North Atlantic and Mediterranean region. SKIRON uses 45 levels in the vertical on a telescopic distribution (from surface to 50 hPa with more layers near the ground) and a time step of 15 s. The outputs of the models are co-located and stored with time frequency of 1 h for the period 2001–2010.

4. RESULTS AND DISCUSSION

4.1. Statistical analysis

The main objective of this study is to present different approaches for the estimation of low wind speed periods based on modeled data. The length of observational time series in the area is not statistically adequate for the evaluation of the methodology. However, similar studies support the use of measurements for such applications.[13] So, despite the fact that the evaluation of the model is not the first priority of this work (it has been performed in other works[33]), a short statistical analysis is included to support the use of it for extreme persistence statistics. Therefore, the purpose of this chapter is not to discuss the model performance in detail but to illustrate some local characteristics and how they are recorded in the model output and observations. In particular, measurements are derived from three different sources. The first is the offshore research platform FINO 1 used for studying environmental conditions for wind power applications in the German North Sea.

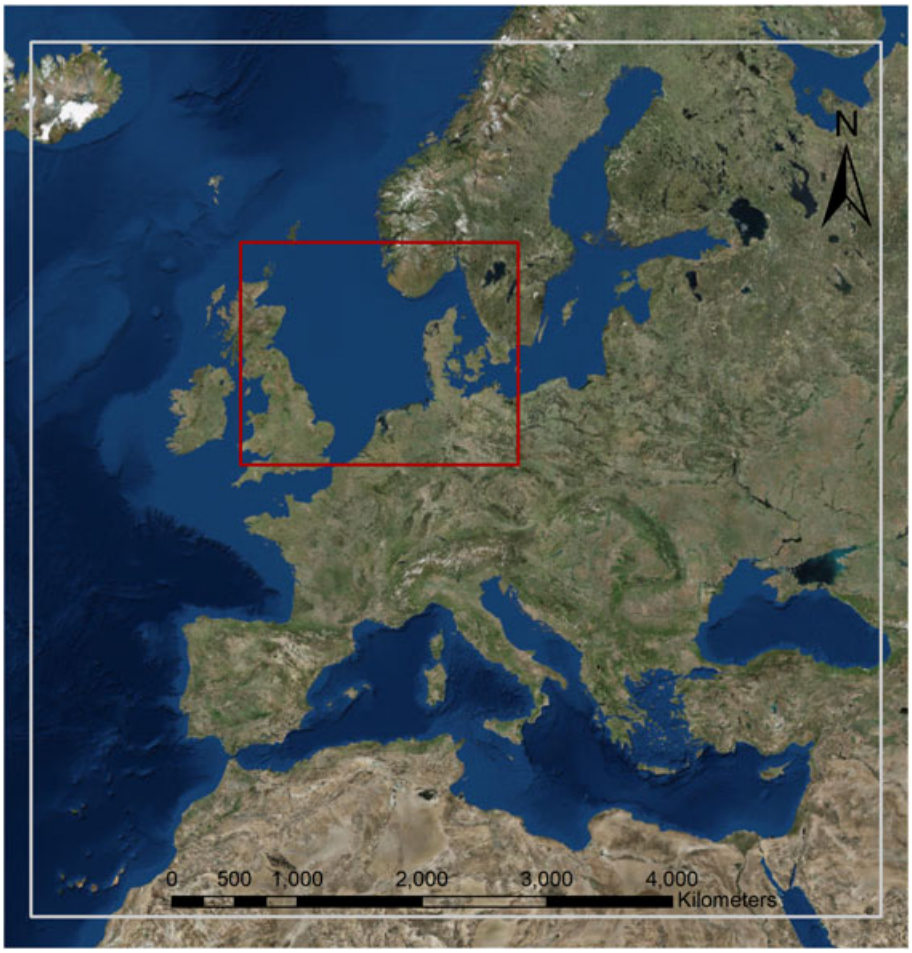

Figure 1. The SKIRON–WAM coupling domain (gray box) and study area (red box). [Colour figure can be viewed at wileyonlinelibrary.com]

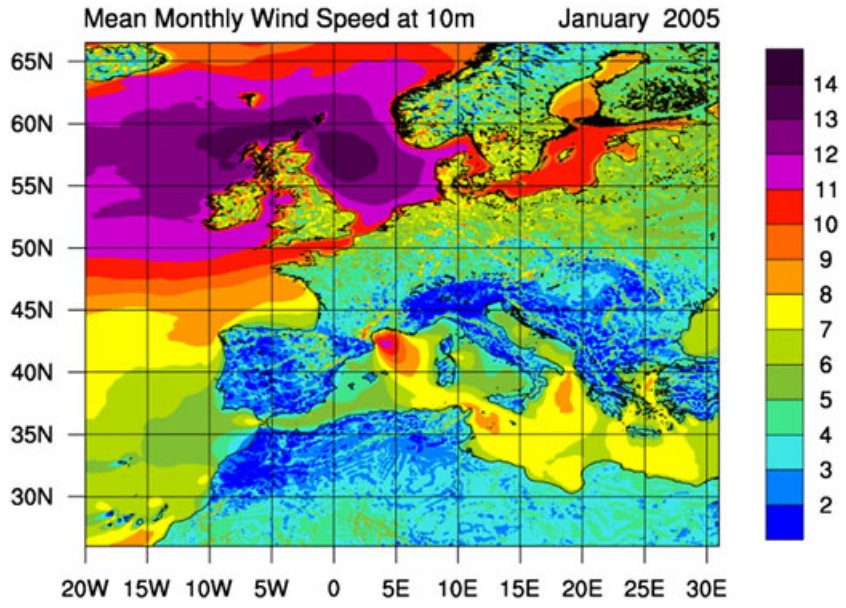

Figure 2. Mean monthly wind speed at 10 m of January 2015. [Colour figure can be viewed at wileyonlinelibrary.com]

The second is the meteorological mast at the site of the Docking Shoal Farm. The third source of measured data is the Greater Gabbard offshore wind farm located around 22 km east of Suffolk coast. The quantity to be evaluated is the 80 m wind speed. The locations of the stations are presented in Figure 3.

It should be noted that modeled parameters are smoothed, during the integration procedure, over the corresponding timestep (15 s in our case). From these values, the model provides/stores outputs on an hourly basis without any further smoothing or averaging. In addition, the observations used are 10 min wind speed averages paired with the modeled data.

Different statistical indexes and graphical analyses were utilized. Coefficient of determination (R^2) is a number that indicates the fit of the modeled data to the measurements. Bias and normalized bias provide information about the systematic deviations between the two data sets. Root mean square error represents the sample standard deviation of the differences between predicted and observed values (it takes also into the consideration the non-systematic errors).[9]

The results of the statistical analysis reveal a rather good agreement between the model and the station for all three cases. In Table I, the basic statistical indexes are provided for the station under consideration. The low bias indicates the non-existence of systematic errors. Higher values (within acceptable limits though) of the other indexes are associated with system noise. The deviation of the two datasets is a result of the smoothing effects associated with the atmospheric model temporal and spatial resolution and physical parameterization. Root mean square error is always high in such model analysis. It is affected by temporal variations and high values and can be attributed among others to phase errors.[34] Such errors are not considered as crucial in our analysis because we focus mainly on the climatic characteristics (long term). The last is the reason why the previous statistical comparison needs to be accompanied with graphs comparing the probability distribution of the samples. To identify the model performance, Q-Q diagrams have been prepared and illustrated in Figure 4.

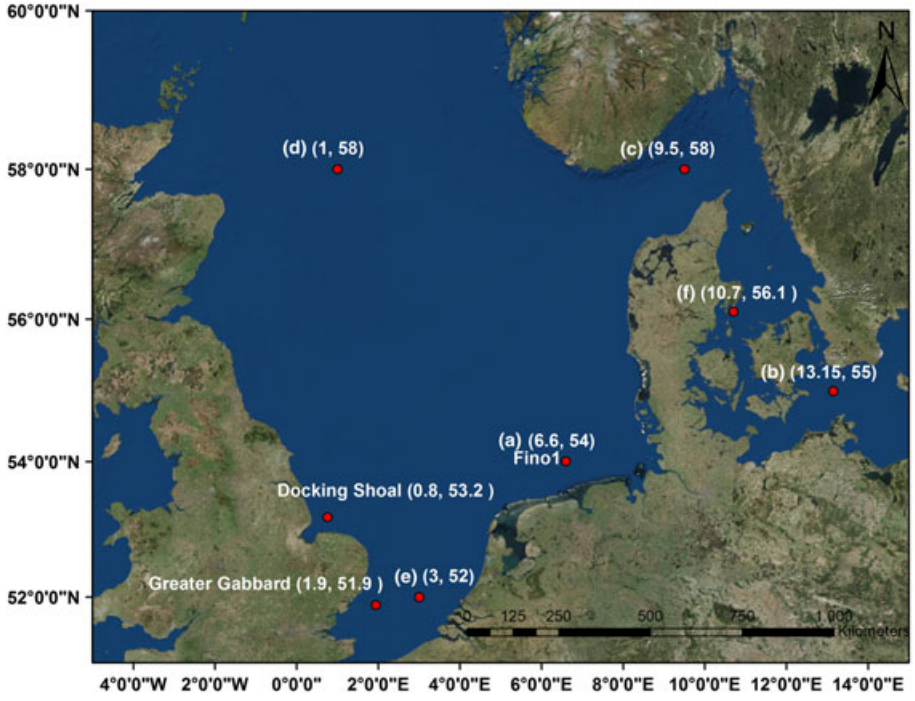

Figure 3. The area of interest and the coordinates of the five selected locations for the application (a, b, c, d, e), the test location for the estimator selection (f) and the offshore platforms FINO 1, Docking Shoal and Greater Gabbard. [Colour figure can be viewed at wileyonlinelibrary.com]

Table I. Statistical analysis of the modeled wind speed against FINO 1, Docking Shoal and Greater Gabbard platforms.

	FINO 1	Docking Shoal	Greater Gabbard
RMSE (m s^{-1})	2.7965	2.613	2.568
Correlation coefficient	0.799	0.821	0.826
R^2	0.638	0.674	0.6823
Bias (m s^{-1})	−0.044	−0.453	−0.472
Normalized bias	0.113	0.052	0.054

RMSE = root mean square error.

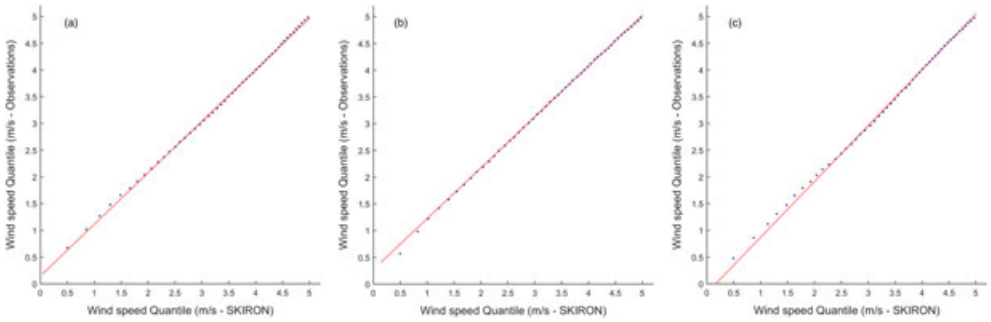

Figure 4. Q-Q plots between Marina database (wind speed—80 m) and FINO 1 (a), Docking Shoal (b) and Greater Gabbard (c) platforms. [Colour figure can be viewed at wileyonlinelibrary.com]

These graphs are focused on low wind speeds as this is the main concern here. As it is seen, the model compares quite well for all cases giving acceptable response.

Issues associated with the modeling capabilities of wind speed in general are well known. The main purpose of this work is not to study wind speed variability but to identify periods of low wind speeds. In order to define the durations of low wind speed events, the wind speed of 3 m s^{-1} was selected because this is the operational threshold for many wind turbines. The total annual events with wind speed below this threshold are presented with respect to their duration (from 2 h to the longest duration) in Figure 5. The year of 2006 of FINO 1 data is chosen as an indicative example because in this case, the missing values of the observations are limited.

It is observed that for the low wind speed, events between the modeled time series and the observations show a good agreement. At the same time an underestimation of the model concerning the short period events is clear, while for longer periods, there is a slight overestimation. The existence of large amounts of missing measurements creates difficulties in this type of comparison as the wind speed down and up-crossings of the selected threshold is a precondition for the definition of low wind speed events. It should also be noted that some types of anemometers face problems measuring such low wind speeds. At the same time, the sampling rate can affect the estimation of the duration of low wind speed events as considered here. However, the errors imported from it are not significant because it is well known that light wind conditions show consistency in terms of intensity.

The lack of availability of at least 10 year measurements with no (or small amount of) missing data causes significant problems in the application of the methodology. This, combined with the fact that the atmospheric models provide the needed parameters in multiple grid points (giving a spatial distribution of them), supports the use of modeled results. So despite the already mentioned differences, the study is based on a mesoscale modeling system

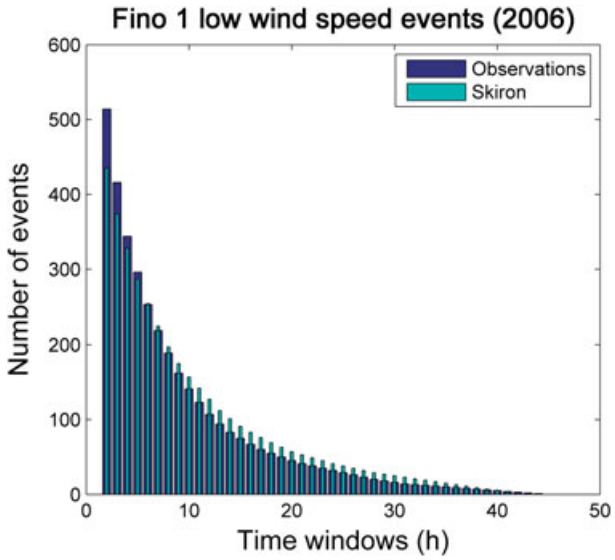

Figure 5. Duration of low wind speed events (<3 m s^{-1}) based on the dataset of Skiron-Marina and the measurements of FINO 1 for the year of 2006. [Colour figure can be viewed at wileyonlinelibrary.com]

database because in the present work, the main objective is to discuss different methodologies and approaches for estimating low wind speed events.

4.2. Intensity given duration approach

4.2.1. Intensity–duration–frequency probability plots.

Low wind speed conditions are always associated with weak pressure gradients encountered often in anticyclonic systems over NE Atlantic and Northern Europe. In addition to the previous discussion, the area under consideration is offshore and rather homogeneous. These facts can lead to the assumption for similar behavior over relatively large regions. Therefore, it is expected that the outcome of the applied methodology from neighboring model grid points should be similar. In this study, five different characteristic areas have been identified and used for further analysis. The selected areas have been chosen according to the mean wind speed, the distance from the coast and the fetching range (Figures 2 and 3). For each of these areas, a square consisting of three consequent points for each side was used (nine points in total).

Using this dataset, probability intensity–duration–frequency analysis was performed. This analysis can be used to estimate the robustness of different techniques for the estimation of the distribution parameters. This can be achieved through the spread of the raw outcome (before the fit of the second-degree polynomial), among the nine neighboring grid points as illustrated via probability plots. The methodology is used for the selection of the better estimator for this area among the MoM and ML. An example of a near-shore location (location f in Figure 3) is depicted in Figure 6. In this case, MoM shows a slight higher deviation concerning the outcome of neighboring points. Apart from the graphical comparison, the values under study have been fitted to a second-degree polynomial, and the corresponding spread is quantified by standard statistical measures (R^2). The previous discussion reveal a slightly better behavior of ML (0.83/0.80), but with a small difference.

In general, bigger differences were found in locations surrounded by land. Considering this, the result could be that MoM may face problems when applied in areas with lower winds. It is known that in light winds, geostrophic control becomes weak, and the land-water distribution becomes relatively more important in determining the wind field. The last can lead to the conclusion that the local climate of near-shore areas may affect the fitting capabilities of MoM and lead to different behavior of neighboring locations. All these come into agreement with previous work[35–37] suggesting that ML method is easily adaptable to include effects of covariates or other influencing factors. For this reason and after a number of corresponding sensitivity tests, it was decided that the ML method is more suitable for this study.

Another important use for the IDF probability graphs would be to quantify uncertainties associated with the spatial distribution of low wind speed events. In this way, the area of interest is described combining the wind speed threshold with the total duration of the event and the probability distribution as confidence interval limits. The probability plots are applied in the fitting curves for the five preselected areas and displayed in Figure 7.

A conclusion that could be reached by taking a closer look to these probability plots is that in case e (the location is shown in Figure 3), there is a relatively large spread that corresponds to a wider confidence interval mainly in higher durations. The reason for this behavior is the location of this area and the specific climatic characteristics as mentioned before. The position is surrounded by land with an open to the North. The land blocks high winds, and therefore, the mean wind speed has smaller values as compared with the North Sea in general. At the same time, local winds dominate the location. As mentioned earlier, in light wind conditions, land-sea interaction becomes considerable and affects the large scale flow.

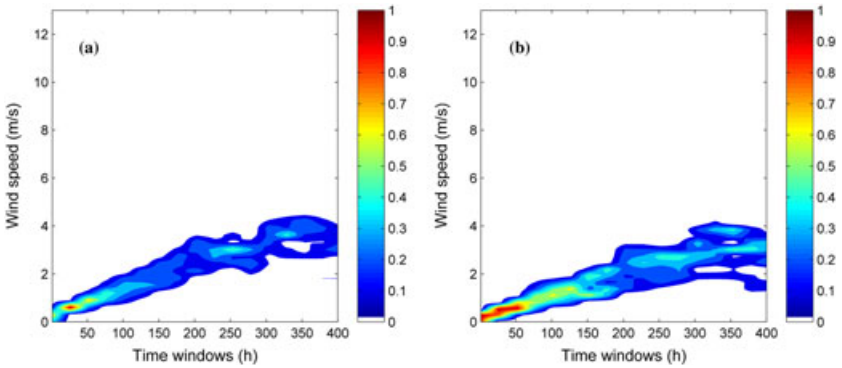

Figure 6. Intensity–duration–frequency probability plots using maximum likelihood (a) and method of moments (b) methodologies (20 year return period) for a near-shore location (10.7 E, 56.1 N—location (f) in Figure 3). [Colour figure can be viewed at wileyonlinelibrary.com]

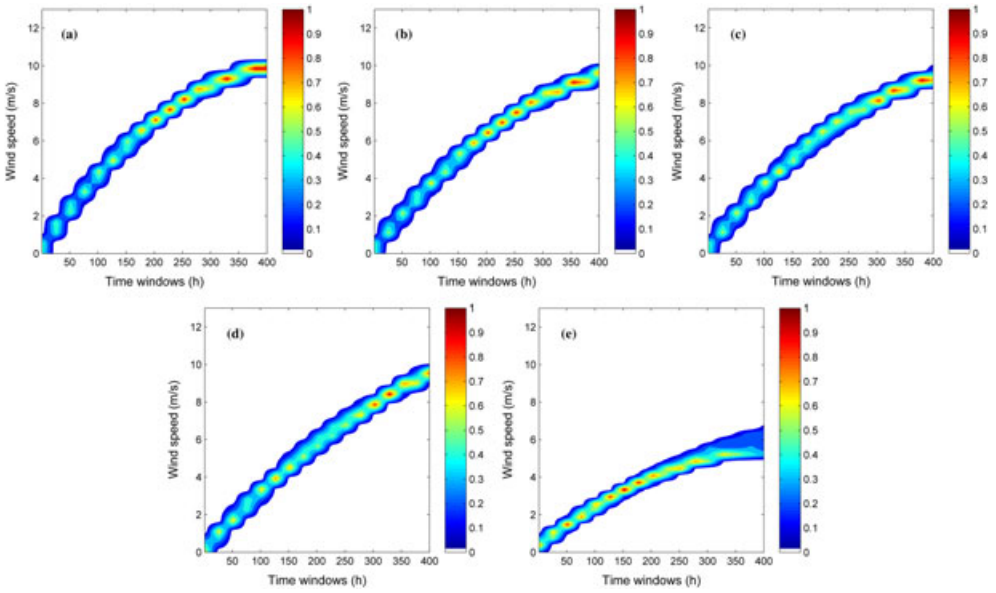

Figure 7. Intensity–duration–frequency probability plots for the five selected locations (20 year return period). [Colour figure can be viewed at wileyonlinelibrary.com]

The influence is more obvious in higher return periods. However, higher deviations are observed in longer durations that correspond to stronger winds. This does not affect the analysis presented in this paper, as lower winds are the main interest. Concluding, it should be noted that a similar procedure could be used for larger areas and more grid points depending on the needs of the study.

4.2.2. Intensity–duration–frequency curves.

The establishment of the relation between the duration, the intensity and the frequency of occurrence of a low wind speed event is represented through the IDF curves. The IDF curves of events associated with wind speed probability distribution lower tail for 20 years return period and the corresponding confidence interval are illustrated in Figure 8. The confidence intervals have been calculated by utilizing the corresponding intervals of the PDF parameters as estimated by the fitting procedure (ML).[13] The curves tend to bend asymptotically, something that was rather expected. For larger time windows, the highest observed speed should be higher but with a decreasing rate. It is also observed that, for point e, the IDF curves reach a maximum value considerably smaller than the other test cases. A conclusion that can be reached is that this area is characterized by low wind speed events that show persistence and/or higher frequency of occurrence as compared with the other test cases. The comparison of the four remaining cases revealed a consistent pattern despite the different local characteristics. However, location d is characterized by a lower curvature. This can be attributed to the fact that it is a deep offshore area, and because there are not land barriers, it is highly exposed to the synoptic systems passage. The synoptic systems of North Atlantic are well known for moving fast and formatting sharp pressure gradients. Locations a, b and c show similar behavior, although it would be expected to observe larger deviations due to the local climate conditions and particularly the sea–land interaction. This shows a persistence in the characteristics of the IDF curves in near shore locations.

The IDF curves for the fourth and fifth test case for different return periods (2, 5, 10, 20 and 50 years) are shown in Figure 9. As expected, the relative positions of the curves with different return periods lead to the conclusion that low wind speed events are less likely to happen for higher durations. From another point of view, such events are expected to last more for higher return periods. At the same time, wind characteristics seem to affect the shape of the IDF curves as the low-wind-speed-event probability of occurrence is obviously higher in the second case (location e).

4.2.3. Spatial distribution of low wind events.

The application of the procedure introduced in the previous steps to the whole area of study led to a series of maps describing the spatial distribution of the three parameters (Equation 5.1) used for the IDF curves. The coefficient of x^2 (α) can take negative values and in some cases values close to zero. In these cases, the parabolic curve part used for the fit of IDF curves is open downward. In some single cases, mainly near shore, the value of α is close to zero, and the curve tends to become linear. The linear coefficient of x (β) takes some negative and more positive values. When the coefficient takes positive values, the line will shift towards the left-bottom and vice versa. The combination of the linear and the nonlinear terms shows how fast the curve will bend and determines the point where the upper wind speed threshold will not change

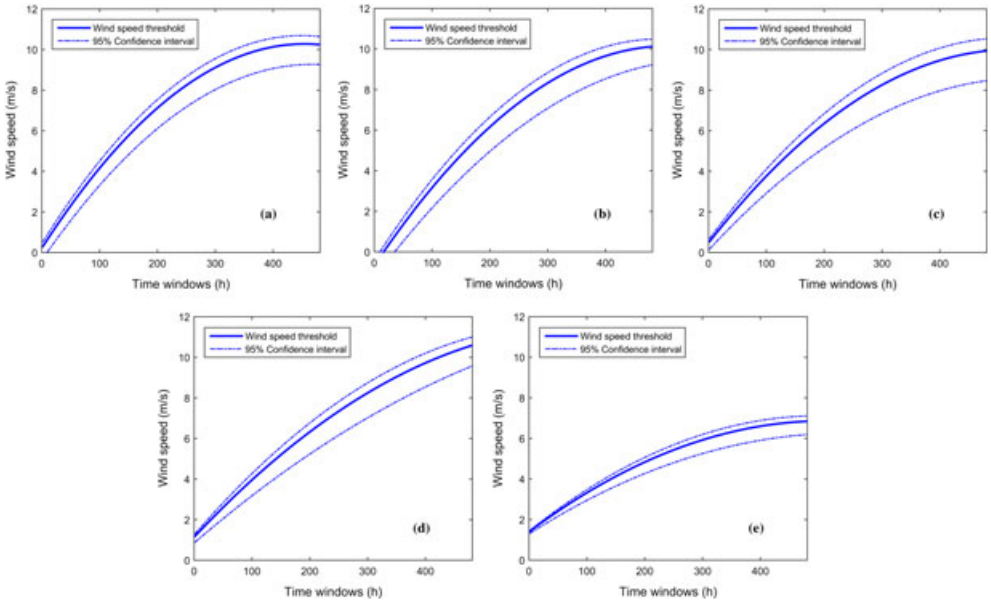

Figure 8. Intensity–duration–frequency curves and the associated confidence intervals for the five selected locations (20 year return period). The confidence intervals have been calculated by utilizing the corresponding intervals of the probability density function parameters as estimated by the fitting procedure (maximum likelihood). The maximum expected wind speed over a low wind speed event is referred here as wind speed threshold to be in conjunction with duration given intensity method. [Colour figure can be viewed at wileyonlinelibrary.com]

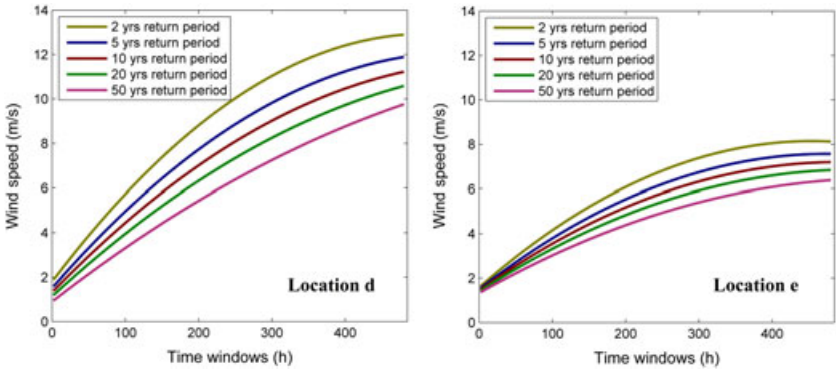

Figure 9. Intensity–duration–frequency curves for locations (d) (left) and (e) (right) and different return periods. [Colour figure can be viewed at wileyonlinelibrary.com]

dramatically for larger time windows. More precisely, the coefficient γ determines whether the curve shifts upward or down. The value of γ is in fact the value where the curve intersects the y-axis. It is obvious that everywhere, it is below the selected threshold of 3 m s^{-1} used for the definition of low wind speed events, which means that such events are more than likely to happen. The negative values mean that the curve will intersect the positive part of x-axis, and wind speed will be constantly close to zero for several hours (for the defined return period). These parameters can be used for the creation of IDF curves throughout the used domain. Their spatial distribution supports the previous discussion and is depicted in Figure 10.

The noticeable spatial distribution of the parameters will change the shape and the characteristics of the IDF curves. These parameters can be used for the solution of the second-degree polynomials for 3 m s^{-1} [$f(x) = 3$], for each point. The outcome is the maximum (statistically) consequent no-energy production period with a recurrence interval of 20 years (Figure 11). It can be easily observed that in the open sea, a low wind speed event can last up to 4–5 days with a recurrence interval set to 20 years. The values rise near shore and reach to more than 10 day periods. This increase is generally expected in gulfs and areas where the wind shadow effect of land affects the wind intensity overseas. At the same time, there are some single cases where low wind speed events can last up to 20 days. This is caused by the interaction of complex

DOI: 10.1002/we

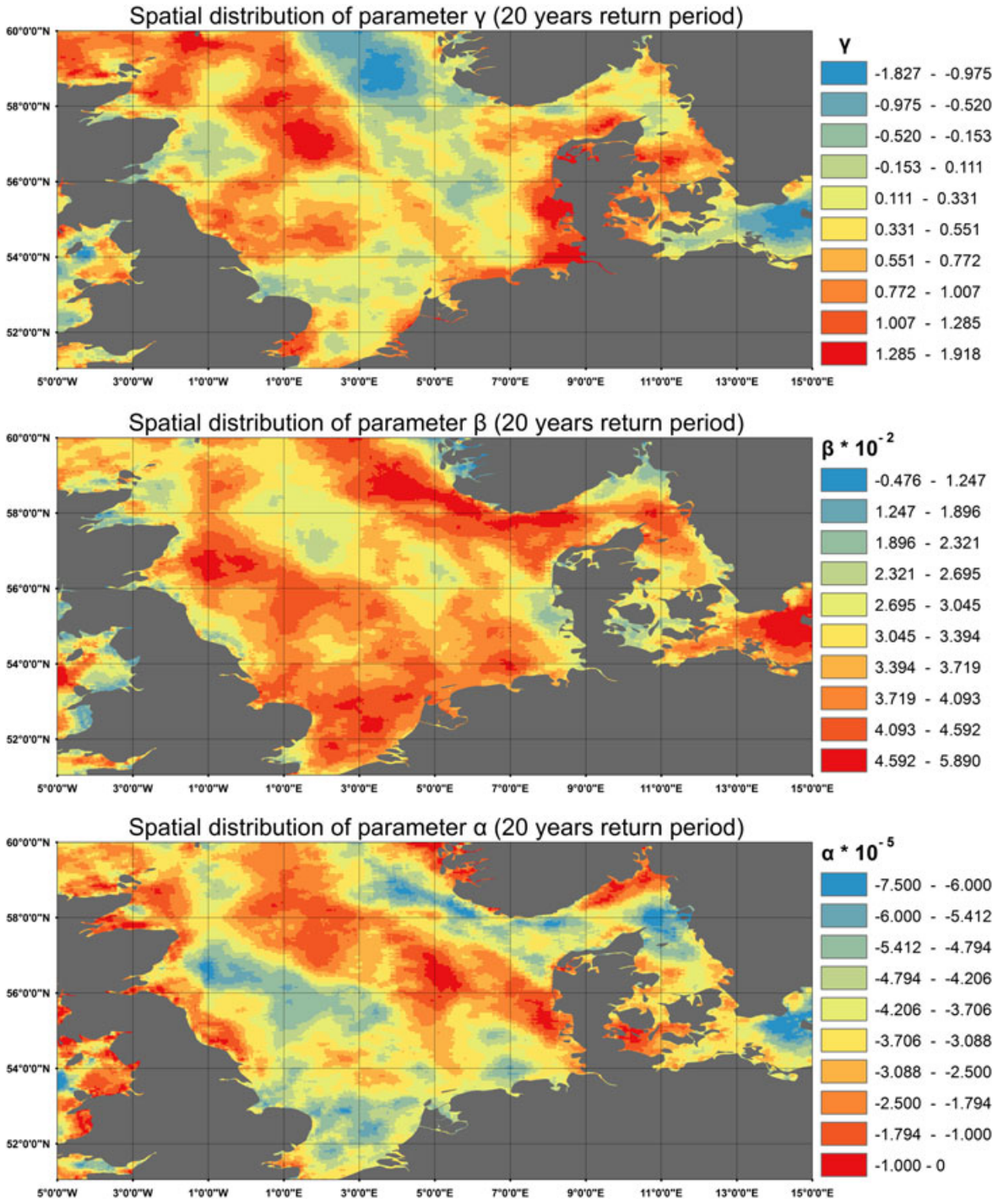

Figure 10. Spatial distribution of the three parameters used for the intensity–duration–frequency curves. [Colour figure can be viewed at wileyonlinelibrary.com]

terrain (with high altitude variations near the shore, especially in the Scandinavian Peninsula) with the atmosphere and the effects of this in the configuration of the model. On one side, the flow near the coast and especially in areas with significant topographic barriers or complex coastline is rather complicated because of dynamical and thermodynamical effects (e.g., channeling, sea-land barriers and boundary layers). On the other side, the mesoscale models fail to reproduce such details in flow structure due to the model resolution used and in general due to the configuration. In this case, the observed discrepancies can be attributed to both.

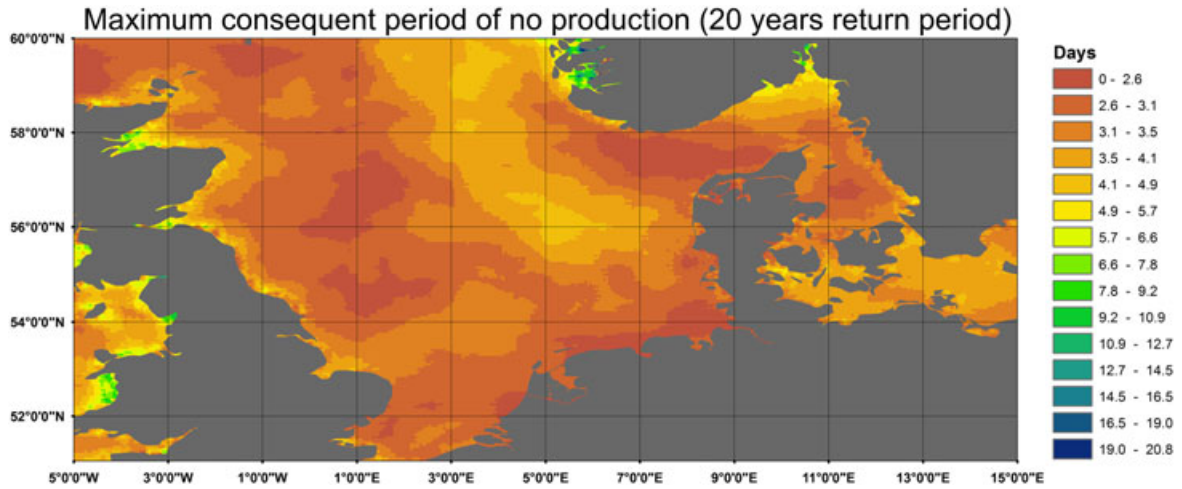

Figure 11. Maximum consequent hours of no energy production with 5% annual probability of occurrence. [Colour figure can be viewed at wileyonlinelibrary.com]

4.2.4. Duration given intensity approach.

For the DGI approach, multiple distributions, such as Gumbel, GEV, Weibull and Rayleigh, were used for the extrapolation of the low wind event duration. The application was made for the five preselected areas used previously. The outcome of IGD approach for the threshold of 3 m s^{-1} is used as a measure for comparison. The results for different return periods are shown in Table II.

For a better understanding of the behavior of the DGI approaches, a normalization based on the IGD methodology was employed and presented in Table III. More specifically, the result is derived as follows: $p = \frac{k_2 - k_1}{k_1} \cdot 100\%$, where k_2 stands for DGI method and k_1 for IGD. It is obvious that both the use of Gumbel and Weibull distribution lead to a constant underestimation as compared with IGD method. This underestimation tends to become more significant in greater return periods and shows a lower exponentiallity. Concerning the application of GEV distribution, there is not a particular pattern on the behavior of the results. The major issue to be mentioned though is that the analysis resulted to up to 80% higher values for the fifth case study. This is a result of the fact that the shape parameter in this case (one of the three parameters to be estimated) is not limited. This is in contrast with Gumbel, for example, where the shape parameter is equal to zero. This can lead to a 'bad' distribution behavior in some cases, depending on the characteristics and the size of the sample. At this point, it should be noticed that in this application, only 10 values were used (annual maxima) that is the lowest limit of the input size recommended for such applications.[14]

Table II. DGI and IGD results (duration in hours) for the selected locations (20, 30, 40 and 50 years return period).

	Duration given intensity								Intensity given duration			
	Gumbel				GEV							
	20 years	30 years	40 years	50 years	20 years	30 years	40 years	50 years	20 years	30 years	40 years	50 years
a	61.4	65.5	68.4	70.6	58.9	62.5	65	67.1	68.1	75.7	81.3	85.9
b	90.5	97	101.5	105.1	97.3	105.7	111.8	116.5	95	106	114	121
c	67	71.1	74	76.3	61	63.1	65.2	66.1	74	84	91	97
d	52.4	55.3	57.4	59	76.5	87.6	96.6	104.3	64.4	73.3	80	86.3
e	55.6	57.5	58.8	59.8	108.7	134.8	157.2	177.7	81.7	88.6	94	98.5
	Weibull				Rayleigh							
	20 years	30 years	40 years	50 years	20 years	30 years	40 years	50 years				
a	59.5	62	63.6	64.8	68.1	72.6	75.6	77.9				
b	85.3	89.1	91.6	93.5	96.1	102.4	106.6	109.8				
c	68	70.8	72.7	74	78.3	83.4	86.9	89.5				
d	46.8	48	48.7	49.3	61.5	65.6	68.3	70.3				
e	50.6	51.2	51.5	51.8	76.9	82	85.4	87.9				

DGI = duration given intensity; GEV = generalized extreme value; IGD = intensity given duration.

DOI: 10.1002/we

Table III. Normalized differences between DGI and IGD results for five locations (20, 30, 40 and 50 years return period).

	Duration Given Intensity							
	Gumbel				GEV			
	20 years (%)	30 years (%)	40 years (%)	50 years (%)	20 years (%)	30 years (%)	40 years (%)	50 years (%)
a	−9.8	−13.5	−15.9	−17.8	−13.5	−17.4	−20.0	−21.9
b	−4.7	−8.5	−11.0	−13.1	2.4	−0.3	−1.9	−3.7
c	−9.5	−15.4	−18.7	−21.3	−17.6	−24.9	−28.4	−31.9
d	−18.6	−24.6	−28.2	−31.6	18.8	19.5	20.78	20.9
e	−32.0	−35.1	−37.4	−39.3	33.0	52.1	67.2	80.4
	Weibull				Rayleigh			
	20 years (%)	30 years (%)	40 years (%)	50 years (%)	20 years (%)	30 years (%)	40 years (%)	50 years (%)
a	−12.6	−18.1	−21.8	−24.6	0.0	−4.1	−7.0	−9.3
b	−10.2	−15.9	−19.6	−22.7	1.2	−3.4	−6.5	−9.3
c	−8.1	−15.7	−20.1	−23.7	5.8	−0.7	−4.5	−7.7
d	−27.3	−34.5	−39.1	−42.9	−4.5	−10.5	−14.6	−18.5
e	−38.1	−42.2	−45.2	−47.4	−5.9	−7.4	−9.1	−10.8

DGI = duration given intensity; GEV = generalized extreme value; IGD = intensity given duration.

Another important issue, which is worth mentioning, is the better results obtained with the use of Rayleigh distribution. The highest difference reaches 18.5%, while for Gumbel (that is a more popular distribution used in AM method and similar applications), it reaches 39.3%. At the same time in most of the cases, the difference is lower than 10% and within the confidence intervals of both methodologies, namely, IGD and DGI. It should be mentioned also that the exponentiality in DGI method is higher if compared with IGD because for higher return periods, the growing ratio is obviously smaller in the first case. Despite the acceptable results, the method is case sensitive, and the use in other areas (with different climatic characteristics) requires a prior analysis similar to the one performed here.

5. CONCLUSIONS

The main objective of this work was to study the duration of the low wind speed events and quantify the associated uncertainties. Two approaches for the quantification were applied and discussed: IGD and DGI. These methods combine the intensity of such events with their duration and their likelihood of occurrence (in terms of return periods). The application of these techniques has as prerequisite the analysis of the suitability of the proposed tools defining their optimum implementation.

The suitability of two different techniques for the distribution parameters estimation, namely, MoM and ML method, was tested alongside with IGD method. The performed tests were based on the assumption that the outcome of the method in neighboring grid points exhibits similar behavior. The results depict the spread of the two methodologies and support the preference of ML.

The relationship between the magnitude and the duration of wind speed for different return periods is made by using IDF curves. The upper and lower bounds are defined using the corresponding parameter estimation confidence intervals and provide a measure of the uncertainties employed in the estimation. These are highly depended on the estimators and the length of the dataset used for the application. In addition, a quantification study of the uncertainties associated with the spatial distribution of the results of the IGD method was attempted by utilizing a probability analysis, based on the IDF curves of neighboring grid points. These results provided the necessary information for the application of IGD method uniformly in a large area. The illustration was made through different maps that depict the spatial distribution of the variables characterizing the IDF curves as well as the consequent hours of no energy production (wind speed below 3 m s^{-1}) with a statistical repeatability that was set to be 20 years long. The main outcomes can be summarized as follows:

- In the open seas, such low wind speed events can last up to 4–5 days.
- Near shore, these periods can reach up to 10 days and in certain cases even more.

Of course, these durations apply for our area under consideration that is the North Sea.

Subsequently, the presented study was focused on the examination of the performance of the GDI methodology by using four different theoretical probability distributions in the application of AM method revealing the following:

- A constant underestimation is observed when using Gumbel and Weibull distribution.
- The application of GEV distribution led to outcome of no particular pattern and large deviations.
- The best results were achieved by using the Rayleigh distribution. The highest difference reaches 18.5%, while in most of the cases, the difference is lower than 10% and within the confidence intervals of both methodologies (IGD and DGI).

It is worth mentioning that the exponentiality in DGI is higher as compared with IGD method, because for higher return periods, the growing ratio is obviously smaller in the first case.

As a concluding remark, it should be noticed that the use of each method and the analysis provided for their comparison give valuable information concerning the local climatic characteristics. The outcome of similar studies could be used to define the probability of occurrence concerning low wind speed events and their effects in the electricity network. The impact of such cases in an economy based on wind energy could be critical. Other renewable energy sources, jointly exploited with wind energy, may support the minimization of such drawbacks.

ACKNOWLEDGEMENTS

The present work was supported by the EU 7th Framework Project MARINA Platform, Grant agreement number: 241402. For the provision of the FINO 1 data, we would like to acknowledge the BMWi (Bundesministerium fuer Wirtschaft und Energie, Federal Ministry for Economic Affairs and Energy) and the PTJ (Projekttraeger Juelich, project executing organization). For the Greater Gabbard and the Docking Shoal data provision, we would like to thank the Crown Estate (Marine data exchange).

REFERENCES

1. Sirnivas S, Musial W, Bailey B, Filippelli M. Assessment of offshore wind system design, safety, and operation standards. Technical Report, NREL/TP-5000-60573, January 2014, Contract No. DE-AC36-08GO28308, 2014.
2. Smith FB. Low wind speed meteorology, for Cambridge atmospheric dispersion modelling course, 6/7 July 1993 – based on the paper presented at Riso in May 1992 and at ECCOMAS, September 1992.
3. Durrans SR. *Intensity-Duration-Frequency Curves, in Rainfall: State of the Science*, Testik F. Y., Gebremichael M. (eds): American Geophys. Union, Washington, D. C., 2010; doi: 10.1029/2009GM000919.
4. Koutsoyiannis D, Kozonis D, Manetas A. A mathematical framework for studying rainfall intensity-duration-frequency relationships. *Journal of Hydrology* 1998; **206**: 118–135.
5. Halwatura D, Lechner AM, Arnold S. Drought severity–duration–frequency curves: a foundation for risk assessment and planning tool for ecosystem establishment in post-mining landscapes. *Hydrology and Earth System Sciences* 2015; **19**: 1069–1091. DOI: 10.5194/hess-19-1069-2015.
6. Sobey RJ, Orloff LS. Intensity-duration-frequency summaries for wave climate. *Coastal Engineering* 1999; **36**: 37–58. DOI: 10.1016/S0378-3839(98)00048-9.
7. Palutikof JP, Brabson BB, Lister DH, Adcock ST. A review of methods to calculate extreme wind speeds. *Meteorological Applications* 1999; **6**: 119–132.
8. Larsén XG, Kalogeri C, Galanis G, Kallos G. A statistical methodology for the estimation of extreme wave conditions for offshore renewable applications. *Renewable Energy* 2015; pp. 205–218. DOI information: 10.1016/j.renene.2015.01.069.
9. Patlakas P, Galanis G, Barranger N, Kallos G. Extreme wind events in a complex maritime environment: ways of quantification. *Journal of Wind Engineering and Industrial Aerodynamics* 2015; **149**: 89–101.
10. Deaves DM, Lines IG. The nature and frequency of low wind-speed conditions. *Journal of Wind Engineering and Industrial Aerodynamics* 1998; **73**: 1–29.
11. Lines IG, Daycock JH, Deaves DM. Guidelines for the inclusion of low wind speed conditions into risk assessments. *Journal of Hazardous Materials* 2001; **83**: 153–179.
12. Gadian A, Dewsbury J, Featherstone F, Levermore J, Morris K, Sanders C. Directional persistence of low wind speed observations. *Journal of Wind Engineering and Industrial Aerodynamics* 2004; **92**: 1061–1074.
13. Leahy P, McKeogh E. Persistence of low wind speed conditions and implications for wind power variability. *Wind Energy* 2012; **2012**: 575–586. DOI: 10.1002/we.1509.

14. Cook NJ. The designer's guide to wind loading of building structures. In *Part 1: Background, Damage Survey, Wind Data and Structural Classification*. Building Research Establishment, Garston, and Butterworths: London, 1985; pp 371.
15. Kallos G, Galanis G, Spyrou C, Kalogeri C, Adam A, Athanasiadis P. Offshore energy mapping for Northeast Atlantic and Mediterranean: MARINA PLATFORM project. Geophys. *Research Abstracts* 2012; **14**: EGU2012–EG10767.
16. Cramér H. *Mathematical Methods of Statistics*. Princeton University Press: Princeton New Jersey, 1946.
17. Kendall MG, Stuart A. *The Advanced Theory of Statistics* (4th edn), vol. **2**. Oxford University Press: New York, 1979.
18. Hazewinkel M. (ed.). *Maximum-Likelihood Method*. Springer: Encyclopedia of Mathematics, 2001. ISBN:978–1–55608-010-4.
19. Hasager CB, Astrup P, Christiansen MB, Nielsen M, Barthelmie R. Wind resources and wind farm wake effects offshore observed from satellite. *Proceedings European Wind Energy Association (EWEA)*, 2006.
20. Kallos G, Kotroni V, Lagouvardos K, Papadopoulos A. On the long-range transport of air pollutants from Europe to Africa. *Geophysical Research Letters* 1998; **25**: 619–622.
21. Kallos G, Astitha M, Katsafados P, Spyrou C. Long-range transport of anthropogenically and naturally produced particulate matter in the Mediterranean and North Atlantic: current state of knowledge. *Journal of Applied Meteorology and Climatology* 2007; **46**: 1230–1251. DOI: 10.1175/JAM2530.1.
22. Spyrou C, Mitsakou C, Kallos G, Louka P, Vlastou G. An improved limited area model for describing the dust cycle in the atmosphere. *Journal of Geophysical Research* 2010; **115**. DOI: 10.1029/2009JD013682 .D172112010
23. Hasselmann S, Hasselmann K, Bauer E, Bertotti L, Cardone CV, Ewing JA, Greenwood JA, Guillaume A, Janssen P, Komen G, Lionello P, Reistad M, Zambresky L. The WAM model – a third generation ocean wave prediction model. *Journal of Physical Oceanography* 1988; **18**: 1775–1810.
24. Galanis G, Chu PC, Kallos G. Statistical post processes for the improvement of the results of numerical wave prediction models. A combination of Kolmogorov-Zurbenko and Kalman filters. *Journal of Operational Oceanography* 2011; **4**: 23–31.
25. Chassignet EP, Smith LT, Halliwell GR, Bleck R. North Atlantic simulations with the hybrid coordinate ocean model (HYCOM): impact of the vertical coordinate choice, reference pressure, and thermobaricity. *Journal of Physical Oceanography* 2003; **33**: 2504–2526.
26. Korres G, Lascaratos A, Hatziapostolou E, Katsafados P. Towards an ocean forecasting system for the Aegean Sea. *Global Atmosphere and Ocean System* 2002; **8**: 191–218.
27. Papadopoulos A, Kallos G, Katsafados P, Nickovic S. The POSEIDON weather forecasting system: an overview. *The Global Atmosphere and Ocean System* 2002; **8**: 219–237.
28. Zodiatis G, Lardner R, Georgiou G, Demirov E, Manzella G, Pinardi N. An operational European global ocean observing system for the eastern Mediterranean Levantine basin: the Cyprus coastal ocean forecasting and observing system. *Marine Technology Society Journal* 2003; **37**: 115–123.
29. Dykes JD, Wang DW, Book JW. An evaluation of a high-resolution operational wave forecasting system in the Adriatic Sea. *Journal of Marine Systems* 2009; **78**: S255–S271.
30. Louka P, Galanis G, Siebert N, Kariniotakis G, Katsafados P, Pytharoulis I, Kallos G. Improvements in wind speed forecasts for wind power prediction purposes using Kalman filtering. *Journal of Wind Engineering and Industrial Aerodynamics* 2008; **96**: 2348–2362.
31. Janeiro J, Martins F, Relvas P. Towards the development of an operational tool for oil spills management in the Algarve coast. *Journal of Coastal Conservation* 2012; **16**: 449–460.
32. Galanis G, Hayes D, Zodiatis G, Chu PC, Kuo YH, Kallos G. Wave characteristics in the Mediterranean Sea by means of numerical modeling, satellite data, statistical and geometrical techniques. *Marine Geophysical Research* 2012; **33**: 1–15.
33. Kalogeri C, Galanis G, Spyrou C, Diamantis D, Baladima F, Koukoula M, Kallos G. Assessing the European offshore wind and wave energy resource for combined exploitation, Ren. *The Energy Journal* 2017; **101**: 244–264.
34. Ardhuin F, Bertotti L, Bidlot J-R, Cavaleri L, Filipetto V, Lefevre J-M, Wittmann P. Comparison of wind and wave measurements and models in the Western Mediterranean Sea. *Ocean Engineering* 2007; **34**: 526–541. DOI: 10.1016/j.oceaneng.2006.02.008.
35. Katz RW, Parlange MB, Naveau P. Statistics of extremes in hydrology. *Advances in Water Resources* 2002; **25**: 1287–1304.
36. Smith RL. Extreme value analysis of environmental time series: An application to trend detection in ground-level ozone. *Statistical Science* 1989; **4**: 367–393.
37. Zhang X, Zwiers FW, Li G. Monte Carlo experiments on the detection of trends in extreme values. *Journal of Climate* 2004; **17**: 1945–1952.